Research and Reviews in Materials Science and Chemistry
Vol. 2, Issue 1, 2013, Pages 1-17
ISSN 2319-6920
Published Online on March 30, 2013

http://jyotiacademicpress.net

INVESTIGATION OF THE EFFECT OF OBLIQUELY INCIDENT DEPOSITION ON STRUCTURAL, MORPHOLOGICAL AND OPTICAL PROPERTIES OF $CuInS_2$ THIN FILMS

A. SINAOUI, F. CHAFFAR AKKARI and M. KANZARI

Laboratoire de Photovoltaïque et Matériaux Semi-conducteurs
Ecole Nationale D'Ingénieurs de Tunis (ENIT)
BP 37, Le belvédère 1002-Tunis
Tunisie
e-mail: azzasinaoui@yahoo.fr

Abstract

$CuInS_2$ thin films were deposited by thermal evaporation method with evaporated obliquely incident deposition technique also known as glancing angle deposition (GLAD) technique. X-ray diffraction (XRD), atomic force microscopy (AFM), and UV-Vis-NIR spectra were used to characterize the structural, surface morphology, and optical properties of the deposited $CuInS_2$ thin films. The surface roughness of GLAD $CuInS_2$ films for the different flux incident angles was studied by two methods AFM and spectrophotometric analysis, which show an increase of surface roughness with increasing of the incident angle. The relationship among the refractive index, packing density, birefringence, and flux incident angle was discussed. We show that the refractive index and the packing density decreased with increasing of the incident angle. The maximum of birefringence (Δn) is up to 0.316 at $\theta = 70^{o}$. The

Keywords and phrases: glancing angle deposition, $CuInS_2$ thin films, surface morphology, packing density, anisotropy, birefringence.

Communicated by Fujun Zhang.

Received July 10, 2012; Revised August 13, 2012

influence of different incident flux angles on the microstructure and optical properties was explored in detail.

1. Introduction

The oblique angle deposition technique also known as glancing angle deposition (GLAD) is a technique for fabricating thin film materials with controlled structure. It is based on thin film deposition by physical vapour deposition and employs oblique angle. Recently, it has attracted a lot of attention in many different applications due to their unique advantages of programmable nanomorphologies [1, 2], thus GLAD technique has been shown to be capable of producing films with various microstructures, such as vertical columns [3], helix [4], and zigzag [5] shape, which is hardly obtained from the normal incidence deposition [6]. Therefore, this technique is an original way to modify many physico-chemical properties of thin films because a wide variety of morphologies can be tailored only with a change of the direction of incident particles flux [1, 2, 7]. GLAD has been also applied successfully to produce porous nanostructures and can exhibit larger anisotropy for some naturally isotropic materials. Natural anisotropic materials often cannot be fabricated as thin films. In this way, the GLAD technique may provide a route to obtain greater optical birefringence [8]. Chalcopyrite semiconductors have been widely regarded as the most promising candidates for absorbers of low cost and high efficiency thin film photovoltaic devices. Among them the ternary compound $CuInS_2$ (CIS), which crystallizes in the chalcopyrite structure. Its physical properties are widely studied. Indeed, its direct band gap of 1.55eV and high absorption coefficient and the environmental viewpoint that $CuInS_2$ does not contain any toxic constituents, in comparison with the frequently studied $CuInSe_2$, make it suitable for terrestrial photovoltaic applications [9, 10].

In this article, we report the microstructure and optical properties of $CuInS_2$ thin films prepared by thermal evaporation method on to glass substrates by using GLAD technique.

The effect of flux incident angle on structural, morphological, and optical properties was investigated. The packing density and in-plane birefringence properties induced by anisotropic structure were also discussed.

2. Experimental Details

2.1. Synthesis of $CuInS_2$

The $CuInS_2$ crystal has been synthesized by direct reaction of high-purity (99.999%) elemental copper, indium, and sulphur. Stoichiometric amounts of the elements Cu, In, and S, corresponding to the composition of the ternary compound, were used to prepare the initial ingot of the $CuInS_2$. The mixture was sealed in a vacuum in a quartz tube. In order to avoid explosions due to sulphur vapour pressure, the quartz tube was heated slowly (20°C/h). A complete homogenization could be obtained by keeping the melt at 1000°C for about 48h. The tube was then cooled at the rate 7°C/h. So the cracking, due to thermal expansion of the melt on solidification, was avoided. X-ray diffraction of $CuInS_2$ powder analysis showed that only the $CuInS_2$ phase was present in the ingot (Figure 2). Crushed powder of this ingot was used as raw material for the thermal evaporation.

2.2. Film preparation

We used a thermal evaporation system to deposit $CuInS_2$ thin films. All the films were deposited onto heated glass substrates of rectangular shape $(2.5 \times 1.5 \text{cm}^2)$ from a tungsten boat by using the GLAD technique without substrate rotation. During our experiments, the substrate was tilted so that the angle between the surface normal of the target and the surface normal of the substrate could be large. The substrate is heated by halogen lamps and the substrate temperature can be varied between room temperature and 180°C during the evaporation process. The deposition by thermal evaporation was performed in a vacuum chamber with a base pressure of 10^{-5} Torr with a diffusion pump. The deposition angle, which was defined to be the angle between the incident flux and

the substrate surface normal was set from θ = 0° to 85°. The substrate temperature (*Ts*) was measured using a thermocouple embedded in the substrate holder underneath the substrates and the target to substrate distance was fixed at 10cm. The glass substrates were previously cleaned with washing agents (commercial detergent, acetone, ethanol, and deionized water) before being introduced into the vacuum system. A schematic drawing of the film deposition system is shown in Figure 1.

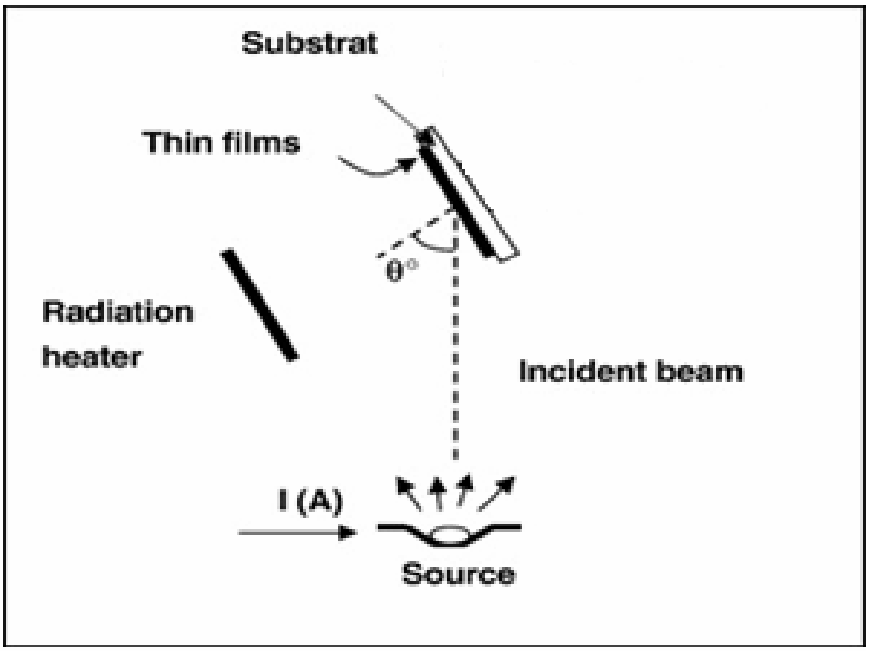

Figure 1. The schematic diagram of the GLAD technique.

2.3. Characterization of the $CuInS_2$ thin films

The crystal structure was characterized by using Philips X'Pert X-Ray diffractometer with a monochromatic CuKα radiation (λ = 0.154056nm). The surface morphology of the films was characterized successively by atomic force microscopy (Veeco Dimension 3100 AFM). The transmittance and reflectance spectra of the GLAD films were measured with an UV-Visible-NIR Shimadzu 3100 S spectrophotometer at normal incidence in the spectral range of 300-1800nm.

3. Results and Discussion

3.1. Structural properties

Figure 2 shows the X-ray diffraction (XRD) patterns of the prepared powder. It is clear that the peak due to the 112 plane has the highest intensity. Indeed, the $CuInS_2$ crystallizes in the chalcopyrite structure with space group (I-42d).

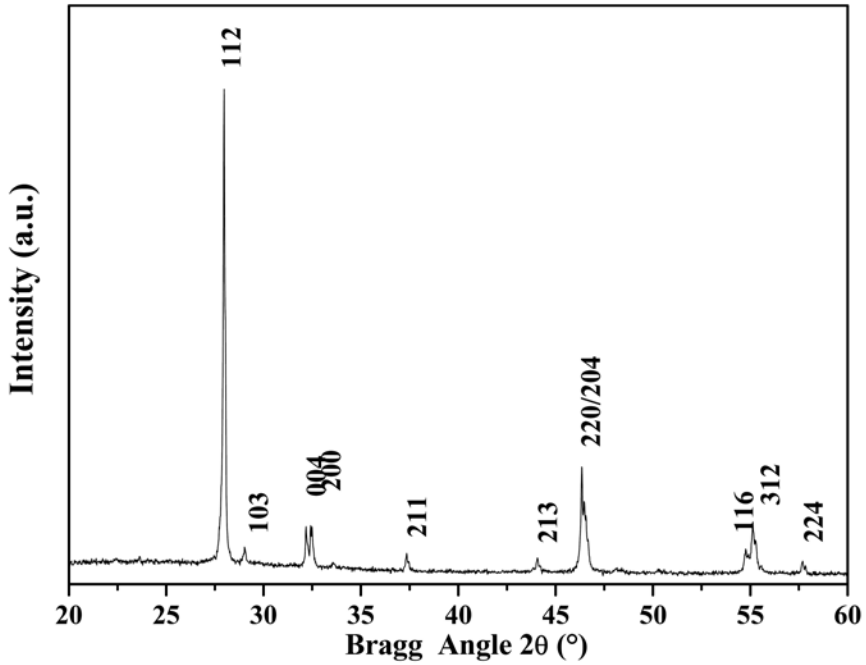

Figure 2. XRD patterns of $CuInS_2$ powder.

The XRD patterns of the GLAD thin films are shown in Figure 3. It is clear from this figure that all the films are polycrystalline. As can be seen, when the incident flux angle θ is low, all diagrams present a peak ($2\theta = 27.9^{o}$), which we have assigned to the 112 plane. We can also note that the intensity of this peak decreases with increasing the incident angle θ. These results are in agreement with the previous works [11, 12].

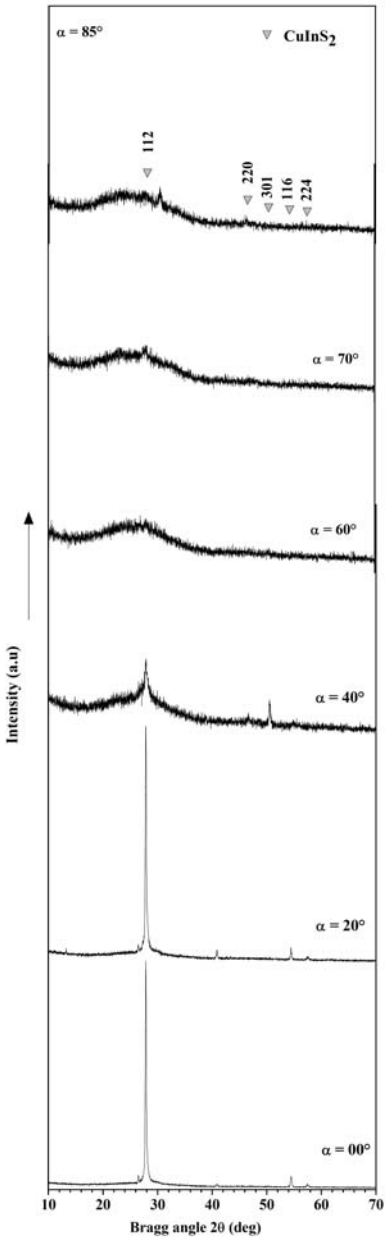

Figure 3. XRD patterns of $CuInS_2$ thin film deposited at different incident angles.

When the films are deposited at high incident flux angle, there is no obvious diffraction peaks indicating that these films present a preponderance amorphous component. The obtained results confirm that, the oblique angle had great effects on the growth of polycrystalline $CuInS_2$ films in particular for the higher oblique angles [13].

3.2. Morphological properties

The morphology of $CuInS_2$ thin films has been investigated by AFM in order to have surface topography information. Figure 4 shows 3D AFM morphological image of $CuInS_2$ thin films deposited at different incident angles from $\theta = 0^o$ to $\theta = 85^o$. As can be seen, the film deposited at $\theta = 85^o$ is constituted of rounded crystallites, which are tilted toward the incident deposition flux.

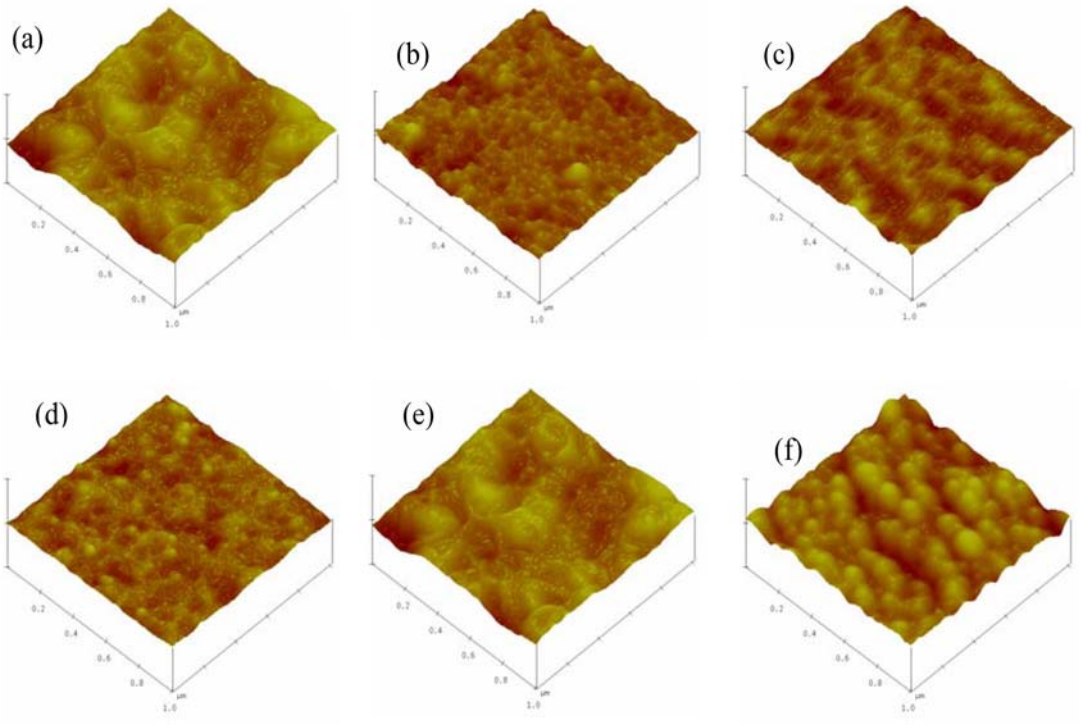

Figure 4. AFM images of $CuInS_2$ films deposited at different incident angles.

It was also observed that the surfaces of the films exhibited a certain degree of roughness and the film became rougher, when the flux incident angle increases. It could be seen that, the root mean square (RMS) values of surface roughness of films were also influenced by the flux angle and increased from 2.1nm at $\theta = 0^{o}$ to 9.4nm at $\theta = 85^{o}$.

The surface roughness parameter of GLAD $CuInS_2$ films was also calculated by using the following formula from the surfaces slightly rough ($\sigma << \lambda$) [14]:

$$R_{sp} = R_{diff} \cdot \left(\frac{4\pi\sigma}{\lambda}\right)^2 \text{ and } R_{diff} = R - R_{sp},$$

where R, R_{diff}, and R_{sp} are the reflection, the diffuse reflection, and the specular reflection, respectively, determined by spectrophotometric analysis from a particular wavelength, σ is the surface roughness parameter.

Variation of surface roughness parameter of $CuInS_2$ films deposited at different incident angles using two methods AFM and spectrophotometric analysis is shown in Figure 5.

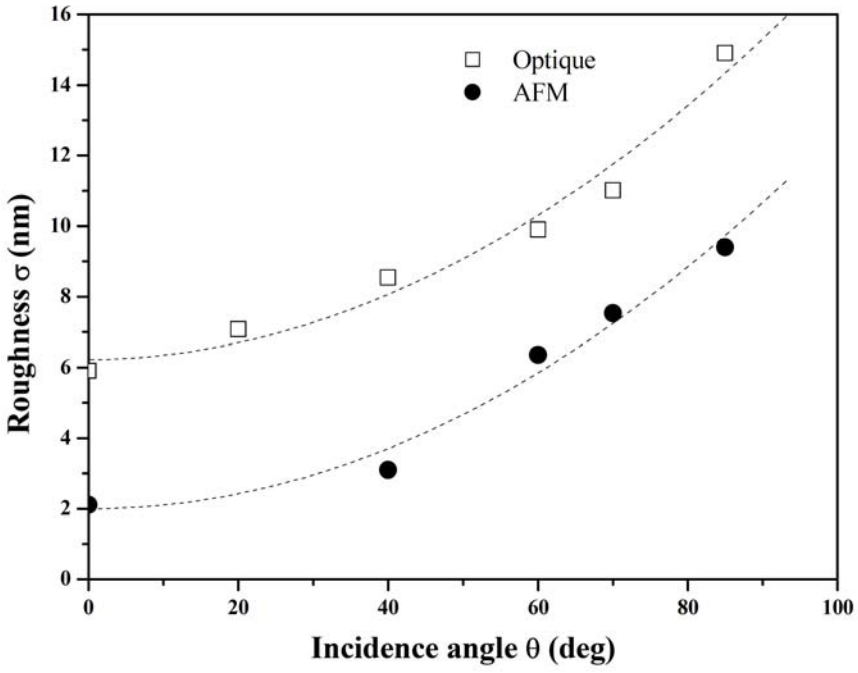

Figure 5. Optical and AFM measurements of surface roughness parameter of $CuInS_2$ thin films.

For both studies, an increase of the surface roughness of the films was observed by increasing the flux incident angle.

3.3. Thickness of the GLAD films

The thickness of the GLAD films varying with the incident flux angle is illustrated in Figure 6.

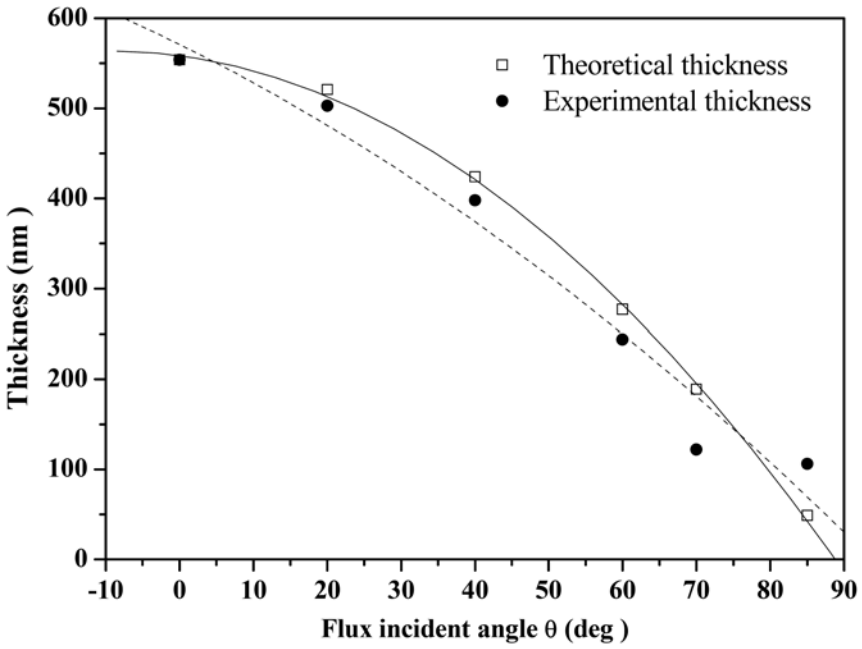

Figure 6. Thickness of $CuInS_2$ thin films varies with the incident flux angle.

The film thickness was calculated from the positions of the interference maxima and minima of reflectance by using a standard method [15]. The thickness of the GLAD films decreases with the increase of incident flux angle. The theoretical thickness t of the GLAD films could be calculated from the following formula [16]:

$$t = t_0 \cos\theta,$$

where t_0 is the nominal thickness. When the incident flux angle θ is low, the thickness of the GLAD films is in agreement with the theoretical thickness. However, the theoretical thickness is larger than the empirical thickness when the incident flux angle θ is high, which can be explained by the inhomogeneity of the films and the porous structure due to the shadowing effect.

3.4. Optical properties

Figure 7 shows the transmittance spectra of $CuInS_2$ films deposited at different incident angles, in the wavelength range 300-1800nm. As can be seen, the transmittance of $CuInS_2$ films decreases gradually as the incident angle increases and at high incident angle, the oscillations are very damped, which can be explained by the shadowing effect and limited adatom diffusion, which inhibits the diffusivity of deposited atoms, thus porous and low density thin films are produced [1].

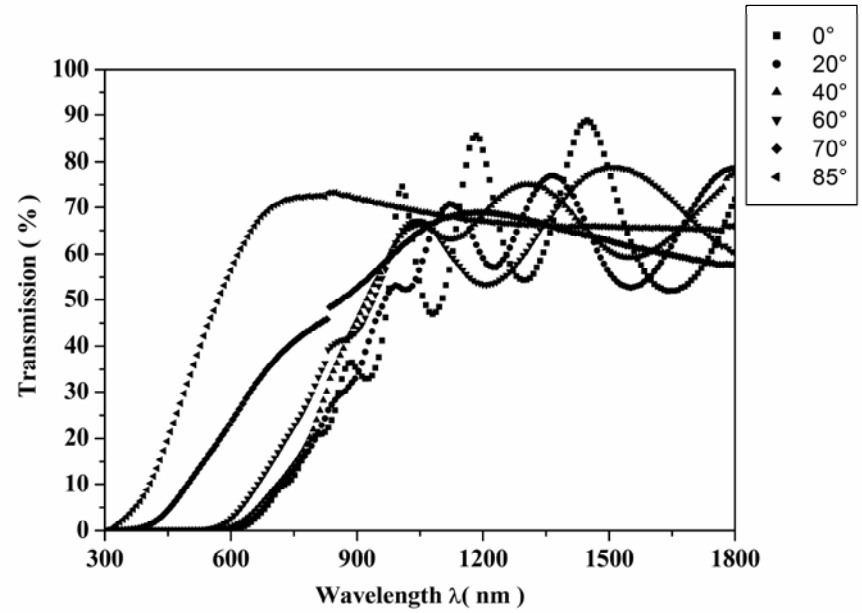

Figure 7. Transmittance spectra of $CuInS_2$ thin films deposited at different incident angles.

We can note also, that the transmittance spectrum shows interference fringes with a sharp fall at the band edge in the region 900-1800nm, whereas the interference effects disappear in the region of very strong absorption, maximum amplitude is obtained in the transparent region.

Based on the transmittance spectra of the $CuInS_2$ thin films, the refractive index of the films was calculated by using modified envelope method [17].

$$n = \left[N + (N^2 - n_0^2 n_1^2)^{\frac{1}{2}} \right]^{\frac{1}{2}},$$

where

$$N = \left[\frac{(n_0^2 + n_1^2)}{2} \right] + 2n_0 n_1 \left[\frac{T_{\max} - T_{\min}}{T_{\max} T_{\min}} \right],$$

where n_0 is the refractive index of air, n_1 is the refractive index of substrate, $T_{\max}$ and $T_{\min}$ are the maximum and minimum transmittances, respectively, for a particular wavelength. Variation of refractive index with wavelength for $CuInS_2$ thin films with different flux incident angle is shown in Figure 8.

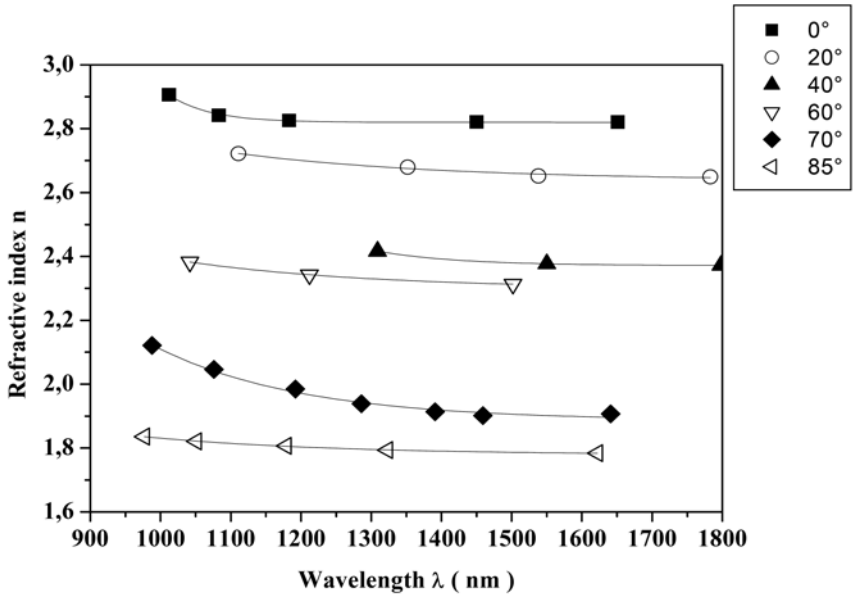

Figure 8. Refractive indices of $CuInS_2$ thin films deposited at different incident angles.

The refractive index of $CuInS_2$ thin films decreases with the increase of deposition angle. At wavelength of λ = 1350nm, the refractive index reduces from 2.819 to 1.792. When the film is deposited with glancing angle deposition, the film becomes a mixture of the film material and air.

The effective packing density of GLAD $CuInS_2$ films can be calculated by using Bruggeman effective medium approximation [18].

$$p_A \frac{\varepsilon_A - \varepsilon}{\varepsilon_A + 2\varepsilon} + p_B \frac{\varepsilon_B - \varepsilon}{\varepsilon_B + 2\varepsilon} = 0,$$

and

$$p_A + p_B = 1,$$

where ε, ε_A, and ε_B are the dielectric functions of the effective medium, material *A*, and material *B*, respectively. p_A and p_B represent the packing density of material *A* and material *B*.

In the field of low absorption, $n^2 >> k^2$ and $\varepsilon = n^2$ (refractive index of $CuInS_2$ deposited at normal incidence), $\varepsilon_A = n_A^2$ (refractive index of $CuInS_2$ deposited at different incident angles), and $\varepsilon_B = n_B^2$ (refractive index of air).

Variation of packing density with flux incident angle for GLAD $CuInS_2$ thin films is shown in Figure 9. The packing density of $CuInS_2$ films decreases with the increase of incident angle.

The relationship between packing density and refractive index are shown in Table 1.

When the incoming flux atoms arrive at the substrate surface normally, the films are compact and the packing density is 1. At incident angle $\theta = 85^o$, the packing density decreases to 0.474, which means that most part of $CuInS_2$ films are filled with air.

The decrease of the refractive index and packing density of GLAD $CuInS_2$ films can be ascribed to the porous structure.

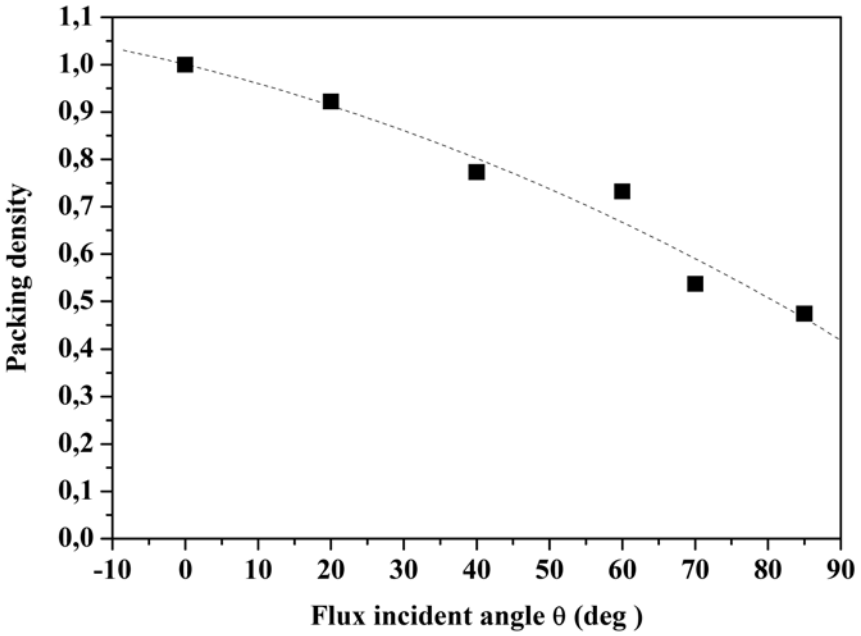

Figure 9. Packing density (λ = 1350nm) of $CuInS_2$ thin films at different deposition angle.

Table 1. Refractive index and packing density of $CuInS_2$ thin films deposited at different flux incident angles

Incidence angle θ (deg)	**Refractive index** (at λ = 1350nm)	**Packing density**
0	2.81	1
20	2.67	0.922
40	2.40	0.773
60	2.32	0.732
70	1.92	0.537
85	1.79	0.474

When transmittance spectra where measured with two orthogonal directions of incident polarized light, in-plane birefringence is defined as the difference between the two refractive indices [19]. Figure 10 illustrates the in-plane birefringence Δn for GLAD $CuInS_2$ films.

The in-plane birefringence increases with the increase of flux incident angle at λ = 1350nm. At $\theta = 70^o$, the birefringence reaches its maximum of Δn = 0.316. Greater flux incident angle results in a decrease of birefringence. It was found that there is a critical packing density for maximum birefringence of GLAD films [20]. We can find that the critical packing density of $CuInS_2$ thin films is about 0.474 at $\theta = 70^o$ (see Table 1). We can deduce that the glancing angle deposition technique is a promising way to obtain larger optical birefringence.

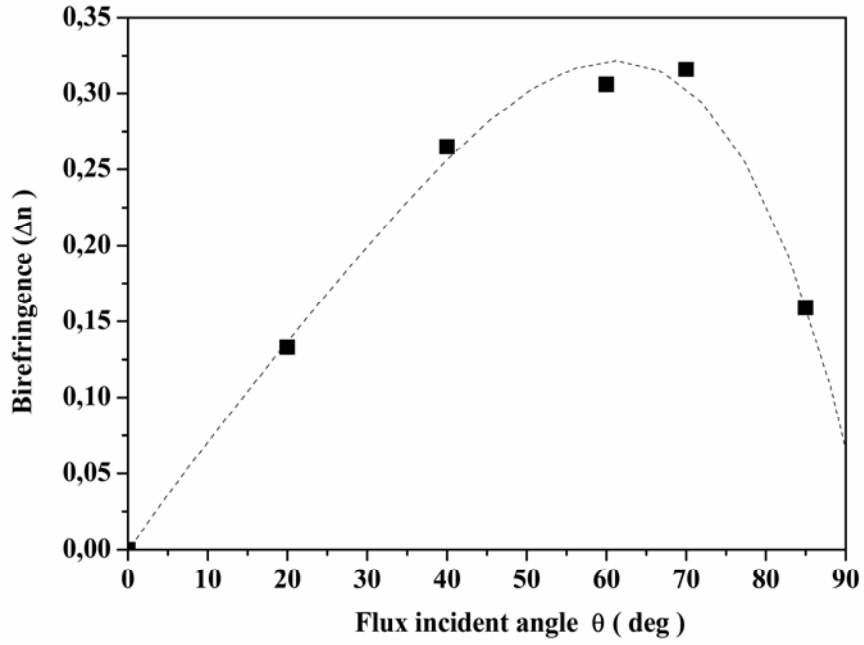

Figure 10. In-plane birefringence Δn (λ = 1350nm) of $CuInS_2$ thin films.

4. Conclusion

$CuInS_2$ thin films were deposited by thermal evaporation method with glancing angle deposition without substrate rotation. The surface roughness parameter increases with the increase of the incident flux incident angle. When the incident angle is high, the theoretical thickness of the GLAD $CuInS_2$ films is greater than the actual thickness, which can be explained by the porous structure. The flux incident angle affects greatly the optical properties of $CuInS_2$ films. As the flux angle increases from 0^o to 85^o, the refractive index of $CuInS_2$ films (at 1350nm) reduces from 2.819 to 1.792 and the packing density reduces from 1 to 0.474. The maximum of birefringence Δn = 0.316 was obtained when the flux incident angle θ is 70^o. These results indicate that the optical properties of GLAD films can be controlled by the GLAD technique, which is a useful method to obtain larger optical birefringence.

References

[1] K. Robbie and M. J. Brett, J. Vac. Sci. Technol. A 15 (1997), 1460.

[2] A. C. Popta, M. M. Hawkeye, J. C. Sit and M. J. Brett, Opt. Lett. 29 (2004), 2545.

[3] B. Dick, M. J. Brett and T. Smy, J. Vac. Sci. Technol. B 21 (2003), 23.

[4] K. Robbie and M. J. Brett, J. Vac. Sci. Technol. A 13 (1995), 2991.

[5] J. Lintymer, N. Martin, J. M. Chappe, P. Delobelle and J. Takadoum, Surf. Coat. Technol. 180-181 (2004), 26.

[6] S. Wang, G. Xia, H. Hea, K. Yia, J. Shao and Z. Fan, Journal of Alloys and Compounds 431 (2007), 287.

[7] J. Lintymer, J. Gavoille, N. Martin and J. Takadoum, Surf. Coat. Technol. 316 (2003), 174.

[8] S. Wang, X. Fu, G. Xia, J. Wang, J. Shao and Z. Fan, Appl. Surf. Sci. 252 (2006), 8734.

[9] M. Zribi, M. Kanzari and B. Rezig, Mater. Lett. 60 (2006), 98.

[10] U. Storkel, M. Aggour, C. P. Murrell and H. J. Lewerenz, Thin Solid Films 387 (2001), 182.

[11] F. Chaffar Akkari, M. Kanzari and B. Rezig, Materials Science and Engineering C 28 (2008), 692.

[12] F. Chaffar Akkari, M. Kanzari and B. Rezig, Physica E 40 (2008), 2577.

[13] F. Chaffar Akkari, R. Brini, M. Kanzari and B. Rezig, Journal of Materials Science 40 (2005), 5751-5755.

[14] http://dx.doi.org/10.1051/bib-sfo:20028032

[15] K. L. Chopra, Thin Film Phenomena, McGraw-Hill, New York, (1969), 721.

[16] K. Wada, M. Yoshiya, N. Yamaguchi and H. Matsubara, Surf. Coat. Technol. 200 (2006), 2725.

[17] R. Swanepoel, J. Phys. E: Sci. Instrum. 16 (1983), 1214.

[18] D. Stroud, Superlattices Microst. 23 (1998), 567.

[19] G. Beydaghyan, K. Kaminska, T. Brown and K. Robbie, Appl. Optic. 43 (2004), 5343.

[20] J. G. Wang, J. D. Shao and Z. X. Fan, Opt. Commun. 247 (2005), 107.

■